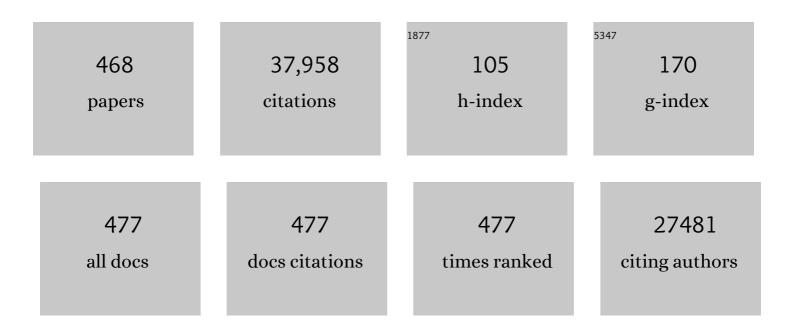
List of Publications by Year in descending order

Source: https://exaly.com/author-pdf/11860499/publications.pdf Version: 2024-02-01



#	Article	IF	CITATIONS
1	Nano-Filamented Textile Sensor Platform with High Structure Sensitivity. ACS Applied Materials & Interfaces, 2022, 14, 15391-15400.	4.0	6
2	Nanocellulose for Sustainable Water Purification. Chemical Reviews, 2022, 122, 8936-9031.	23.0	82
3	Nanostructured all-cellulose membranes for efficient ultrafiltration of wastewater. Journal of Membrane Science, 2022, 650, 120422.	4.1	20
4	Biodegradable silk fibroin-based bio-piezoelectric/triboelectric nanogenerators as self-powered electronic devices. Nano Energy, 2022, 96, 107101.	8.2	41
5	Nanocellulose in membrane technology for water purification. Separation Science and Technology, 2022, , 69-85.	0.0	0
6	Plant-derived carboxycellulose: Highly efficient bionanomaterials for removal of toxic lead from contaminated water. Separation Science and Technology, 2022, , 87-95.	0.0	0
7	Nitro-oxidation process for fabrication of efficient bioadsorbent from lignocellulosic biomass by combined liquid-gas phase treatment. Carbohydrate Polymer Technologies and Applications, 2022, 3, 100219.	1.6	0
8	Nitro-oxidized carboxylated cellulose nanofiber based nanopapers and their PEM fuel cell performance. Sustainable Energy and Fuels, 2022, 6, 3669-3680.	2.5	11
9	Elucidating the Opportunities and Challenges for Nanocellulose Spinning. Advanced Materials, 2021, 33, e2001238.	11.1	43
10	Integrated dynamic wet spinning of core-sheath hydrogel fibers for optical-to-brain/tissue communications. National Science Review, 2021, 8, nwaa209.	4.6	36
11	Antifouling nanocellulose membranes: How subtle adjustment of surface charge lead to self-cleaning property. Journal of Membrane Science, 2021, 618, 118739.	4.1	46
12	Sequential Oxidation on Wood and Its Application in Pb2+ Removal from Contaminated Water. Polysaccharides, 2021, 2, 245-256.	2.1	5
13	Electrospun Nanofibrous Adsorption Membranes for Wastewater Treatment: Mechanical Strength Enhancement. Chemical Research in Chinese Universities, 2021, 37, 355-365.	1.3	7
14	The Influence of Ethyl Branch on Formation of Shish-Kebab Crystals in Bimodal Polyethylene under Shear at Low Temperature. Chinese Journal of Polymer Science (English Edition), 2021, 39, 1050-1058.	2.0	4
15	Crystal structural evolution of Polybutene-1 in solid state upon deformation and stress relaxation. Polymer, 2021, 226, 123833.	1.8	1
16	Nitro-oxidized carboxycellulose nanofibers from moringa plant: effective bioadsorbent for mercury removal. Cellulose, 2021, 28, 8611-8628.	2.4	26
17	Shear-induced crystallization of unimodal/bimodal polyethylene at high temperatures affected by C4 short-branching. Polymer, 2021, 233, 124203.	1.8	3
18	Enhanced anti-fouling performance in Membrane Bioreactors using a novel cellulose nanofiber-coated membrane. Separation and Purification Technology, 2021, 275, 119145.	3.9	19

#	Article	IF	CITATIONS
19	Understanding ion-induced assembly of cellulose nanofibrillar gels through shear-free mixing and in situ scanning-SAXS. Nanoscale Advances, 2021, 3, 4940-4951.	2.2	5
20	Shear-free mixing to achieve accurate temporospatial nanoscale kinetics through scanning-SAXS: ion-induced phase transition of dispersed cellulose nanocrystals. Lab on A Chip, 2021, 21, 1084-1095.	3.1	6
21	Lamellar crystal-dominated surfaces of polymer films achieved <i>via</i> melt stretching-induced free surface crystallization. Soft Matter, 2021, 17, 10829-10838.	1.2	1
22	Study the Use of Activated Carbon and Bone Char on the Performance of Gravity Sand-Bag Water Filter. Membranes, 2021, 11, 868.	1.4	5
23	Functionalized bioâ€adsorbents for removal of perfluoroalkyl substances: A perspective. AWWA Water Science, 2021, 3, .	1.0	8
24	Highly permeable nanofibrous composite microfiltration membranes for removal of nanoparticles and heavy metal ions. Separation and Purification Technology, 2020, 233, 115976.	3.9	72
25	Highly efficient and sustainable carboxylated cellulose filters for removal of cationic dyes/heavy metals ions. Chemical Engineering Journal, 2020, 389, 123458.	6.6	88
26	Engineering construction of robust superhydrophobic two-tier composite membrane with interlocked structure for membrane distillation. Journal of Membrane Science, 2020, 598, 117813.	4.1	41
27	Heparinized thin-film composite membranes with sub-micron ridge structure for efficient hemodialysis. Journal of Membrane Science, 2020, 599, 117706.	4.1	25
28	Cross-Sections of Nanocellulose from Wood Analyzed by Quantized Polydispersity of Elementary Microfibrils. ACS Nano, 2020, 14, 16743-16754.	7.3	45
29	Surfaceâ€Mediated Interconnections of Nanoparticles in Cellulosic Fibrous Materials toward 3D Sensors. Advanced Materials, 2020, 32, e2002171.	11.1	18
30	Rice husk based nanocellulose scaffolds for highly efficient removal of heavy metal ions from contaminated water. Environmental Science: Water Research and Technology, 2020, 6, 3080-3090.	1.2	30
31	Remediation of UO <sub>2</sub> <sup>2+</sup> from Water by Nitro-Oxidized Carboxycellulose Nanofibers: Performance and Mechanism. ACS Symposium Series, 2020, , 269-283.	0.5	7
32	High-flux anti-fouling nanofibrous composite ultrafiltration membranes containing negatively charged water channels. Journal of Membrane Science, 2020, 612, 118382.	4.1	17
33	Hierarchical Assembly of Nanocellulose into Filaments by Flow-Assisted Alignment and Interfacial Complexation: Conquering the Conflicts between Strength and Toughness. ACS Applied Materials & Interfaces, 2020, 12, 32090-32098.	4.0	29
34	Cationic Dialdehyde Nanocellulose from Sugarcane Bagasse for Efficient Chromium(VI) Removal. ACS Sustainable Chemistry and Engineering, 2020, 8, 4734-4744.	3.2	58
35	Ultra-fine electrospun nanofibrous membranes for multicomponent wastewater treatment: Filtration and adsorption. Separation and Purification Technology, 2020, 242, 116794.	3.9	53
36	Membrane Bioreactors for Nitrogen Removal from Wastewater: A Review. Journal of Environmental Engineering, ASCE, 2020, 146, .	0.7	26

#	Article	IF	CITATIONS
37	Nanocelluloseâ€Enabled Membranes for Water Purification: Perspectives. Advanced Sustainable Systems, 2020, 4, 1900114.	2.7	118
38	Facile synthesis of TiO2/CNC nanocomposites for enhanced Cr(VI) photoreduction: Synergistic roles of cellulose nanocrystals. Carbohydrate Polymers, 2020, 233, 115838.	5.1	43
39	Reinforcement of Natural Rubber Latex Using Jute Carboxycellulose Nanofibers Extracted Using Nitro-Oxidation Method. Nanomaterials, 2020, 10, 706.	1.9	24
40	Cellulose nanofibrils and nanocrystals in confined flow: Single-particle dynamics to collective alignment revealed through scanning small-angle x-ray scattering and numerical simulations. Physical Review E, 2020, 101, 032610.	0.8	26
41	Sustainable carboxylated cellulose filters for efficient removal and recovery of lanthanum. Environmental Research, 2020, 188, 109685.	3.7	18
42	Strong Silk Fibers Containing Cellulose Nanofibers Generated by a Bioinspired Microfluidic Chip. ACS Sustainable Chemistry and Engineering, 2019, 7, 14765-14774.	3.2	42
43	Enhancing Dehydration Performance of Isopropanol by Introducing Intermediate Layer into Sodium Alginate Nanofibrous Composite Pervaporation Membrane. Advanced Fiber Materials, 2019, 1, 137-151.	7.9	15
44	Morphology and Flow Behavior of Cellulose Nanofibers Dispersed in Glycols. Macromolecules, 2019, 52, 5499-5509.	2.2	18
45	Operation of proton exchange membrane (PEM) fuel cells using natural cellulose fiber membranes. Sustainable Energy and Fuels, 2019, 3, 2725-2732.	2.5	28
46	The influence of short chain branch on formation of shear-induced crystals in bimodal polyethylene at low shear temperatures. Polymer, 2019, 179, 121625.	1.8	9
47	Colorful nanofibrous composite membranes by two-nozzle electrospinning. Materials Today Communications, 2019, 21, 100643.	0.9	4
48	Silver Nanoparticle-Enabled Photothermal Nanofibrous Membrane for Light-Driven Membrane Distillation. Industrial & Engineering Chemistry Research, 2019, 58, 3269-3281.	1.8	70
49	Structural characterization of carboxyl cellulose nanofibers extracted from underutilized sources. Science China Technological Sciences, 2019, 62, 971-981.	2.0	18
50	Synthesis and Characterization of a High Flux Nanocellulose–Cellulose Acetate Nanocomposite Membrane. Membranes, 2019, 9, 70.	1.4	25
51	Interpenetrating Nanofibrous Composite Membranes for Water Purification. ACS Applied Nano Materials, 2019, 2, 3606-3614.	2.4	24
52	Effective chromium removal from water by polyaniline-coated electrospun adsorbent membrane. Chemical Engineering Journal, 2019, 372, 341-351.	6.6	151
53	Novel thin-film nanofibrous composite membranes containing directional toxin transport nanochannels for efficient and safe hemodialysis application. Journal of Membrane Science, 2019, 582, 151-163.	4.1	43
54	Influences of tacticity and molecular weight on crystallization kinetic and crystal morphology under isothermal crystallization: Evidence of tapering in lamellar width. Polymer, 2019, 172, 41-51.	1.8	14

#	Article	IF	CITATIONS
55	Robust superhydrophobic dual layer nanofibrous composite membranes with a hierarchically structured amorphous polypropylene skin for membrane distillation. Journal of Materials Chemistry A, 2019, 7, 11282-11297.	5.2	52
56	Electrospun Nanofibrous Membranes for Desalination. , 2019, , 81-104.		13
57	Efficient Removal of Arsenic Using Zinc Oxide Nanocrystal-Decorated Regenerated Microfibrillated Cellulose Scaffolds. ACS Sustainable Chemistry and Engineering, 2019, 7, 6140-6151.	3.2	93
58	Biofouling-resistant nanocellulose layer in hierarchical polymeric membranes: Synthesis, characterization and performance. Journal of Membrane Science, 2019, 579, 162-171.	4.1	40
59	Arsenic(III) Removal by Nanostructured Dialdehyde Cellulose–Cysteine Microscale and Nanoscale Fibers. ACS Omega, 2019, 4, 22008-22020.	1.6	66
60	A study of TiO <sub>2</sub> nanocrystal growth and environmental remediation capability of TiO <sub>2</sub> /CNC nanocomposites. RSC Advances, 2019, 9, 40565-40576.	1.7	29
61	Enhanced pervaporation performance of polyamide membrane with synergistic effect of porous nanofibrous support and trace graphene oxide lamellae. Chemical Engineering Science, 2019, 196, 265-276.	1.9	33
62	A thirst for advancement. Nature Materials, 2018, 17, 213-215.	13.3	1
63	Nanocellulose Extracted from Defoliation of Ginkgo Leaves. MRS Advances, 2018, 3, 2077-2088.	0.5	11
64	Sulfonylcalix[4]arene functionalized nanofiber membranes for effective removal and selective fluorescence recognition of terbium( <scp>iii</scp> ) ions. New Journal of Chemistry, 2018, 42, 6191-6202.	1.4	7
65	The influence of short chain branch on formation of shishâ€kebab crystals in bimodal polyethylene under shear at high temperatures. Journal of Polymer Science, Part B: Polymer Physics, 2018, 56, 786-794.	2.4	12
66	Integrated polyamide thin-film nanofibrous composite membrane regulated by functionalized interlayer for efficient water/isopropanol separation. Journal of Membrane Science, 2018, 553, 70-81.	4.1	67
67	Lead removal from water using carboxycellulose nanofibers prepared by nitro-oxidation method. Cellulose, 2018, 25, 1961-1973.	2.4	69
68	Understanding the Mechanistic Behavior of Highly Charged Cellulose Nanofibers in Aqueous Systems. Macromolecules, 2018, 51, 1498-1506.	2.2	92
69	Nanocellulose from Spinifex as an Effective Adsorbent to Remove Cadmium(II) from Water. ACS Sustainable Chemistry and Engineering, 2018, 6, 3279-3290.	3.2	138
70	An unusual promotion of Î <sup>3</sup> -crystals in metallocene-made isotactic polypropylene from orientational relaxation and favorable temperature window induced by shear. Polymer, 2018, 134, 196-203.	1.8	14
71	The influence of short chain branch on formation of shear induced crystals in bimodal polyethylene at high shear temperatures. European Polymer Journal, 2018, 105, 359-369.	2.6	13
72	Effect of Sorbitol Templates on the Preferential Crystallographic Growth of Isotactic Polypropylene Wax. Crystals, 2018, 8, 59.	1.0	1

#	Article	IF	CITATIONS
73	Anionic Surfactant-Triggered Steiner Geometrical Poly(vinylidene fluoride) Nanofiber/Nanonet Air Filter for Efficient Particulate Matter Removal. ACS Applied Materials & Interfaces, 2018, 10, 42891-42904.	4.0	73
74	Single Molecular Layer of Silk Nanoribbon as Potential Basic Building Block of Silk Materials. ACS Nano, 2018, 12, 11860-11870.	7.3	79
75	Nanocomposite Film Containing Fibrous Cellulose Scaffold and Ag/TiO2 Nanoparticles and Its Antibacterial Activity. Polymers, 2018, 10, 1052.	2.0	22
76	Eco-friendly poly(acrylic acid)-sodium alginate nanofibrous hydrogel: A multifunctional platform for superior removal of Cu(II) and sustainable catalytic applications. Colloids and Surfaces A: Physicochemical and Engineering Aspects, 2018, 558, 228-241.	2.3	74
77	Current Advances on Nanofiber Membranes for Water Purification Applications. , 2018, , 25-46.		10
78	Self-roughened omniphobic coatings on nanofibrous membrane for membrane distillation. Separation and Purification Technology, 2018, 206, 14-25.	3.9	82
79	High Aspect Ratio Carboxycellulose Nanofibers Prepared by Nitro-Oxidation Method and Their Nanopaper Properties. ACS Applied Nano Materials, 2018, 1, 3969-3980.	2.4	47
80	Shear induced crystallization of bimodal and unimodal high density polyethylene. Polymer, 2018, 153, 223-231.	1.8	6
81	Ultra-strong, tough and high wear resistance high-density polyethylene for structural engineering application: A facile strategy towards using the combination of extensional dynamic oscillatory shear flow and ultra-high-molecular-weight polyethylene. Composites Science and Technology, 2018, 167, 301-312.	3.8	29
82	Modification of carbon nanotubes with fluorinated ionic liquid for improving processability of fluoro-ethylene-propylene. European Polymer Journal, 2017, 87, 398-405.	2.6	17
83	Sequence distribution and elastic properties of propylene-based elastomers. Polymer, 2017, 111, 115-122.	1.8	13
84	Characterization of Nanocellulose Using Small-Angle Neutron, X-ray, and Dynamic Light Scattering Techniques. Journal of Physical Chemistry B, 2017, 121, 1340-1351.	1.2	112
85	Interfacial Shish-Kebabs Lengthened by Coupling Effect of In Situ Flexible Nanofibrils and Intense Shear Flow: Achieving Hierarchy To Conquer the Conflicts between Strength and Toughness of Polylactide. ACS Applied Materials & Interfaces, 2017, 9, 10148-10159.	4.0	77
86	A durable thin-film nanofibrous composite nanofiltration membrane prepared by interfacial polymerization on a double-layer nanofibrous scaffold. RSC Advances, 2017, 7, 18001-18013.	1.7	39
87	Comprehensive study on temperature-induced crystallisation and strain-induced crystallisation behaviours of natural rubber/isoprene rubber blends. Plastics, Rubber and Composites, 2017, 46, 290-300.	0.9	5
88	Superior Impact Toughness and Excellent Storage Modulus of Poly(lactic acid) Foams Reinforced by Shish-Kebab Nanoporous Structure. ACS Applied Materials & Interfaces, 2017, 9, 21071-21076.	4.0	69
89	Super-hydrophobic modification of porous natural polymer "luffa sponge―for oil absorption. Polymer, 2017, 126, 470-476.	1.8	52
90	Ionic Cross-Linked Poly(acrylonitrile- <i>co</i> -acrylic acid)/Polyacrylonitrile Thin Film Nanofibrous Composite Membrane with High Ultrafiltration Performance. Industrial & Engineering Chemistry Research, 2017, 56, 3077-3090.	1.8	17

#	Article	IF	CITATIONS
91	Rheological Properties of Jute-Based Cellulose Nanofibers under Different Ionic Conditions. ACS Symposium Series, 2017, , 113-132.	O.5	8
92	Structure characterization of cellulose nanofiber hydrogel as functions of concentration and ionic strength. Cellulose, 2017, 24, 5417-5429.	2.4	59
93	A Criterion for Flowâ€Induced Oriented Crystals in Isotactic Polypropylene under Pressure. Macromolecular Rapid Communications, 2017, 38, 1700407.	2.0	12
94	Efficient Removal of UO <sub>2</sub> <sup>2+</sup> from Water Using Carboxycellulose Nanofibers Prepared by the Nitro-Oxidation Method. Industrial & Engineering Chemistry Research, 2017, 56, 13885-13893.	1.8	79
95	Decoration of Nanofibrous Paper Chemiresistors with Dendronized Nanoparticles toward Structurally Tunable Negativeâ€Going Response Characteristics to Human Breathing and Sweating. Advanced Materials Interfaces, 2017, 4, 1700380.	1.9	15
96	Nanoparticle Based Printed Sensors on Paper for Detecting Chemical Species. , 2017, , .		6
97	Deformation X-ray study of propylene-based elastomers with controlled sequence distributions. Polymer, 2017, 122, 208-221.	1.8	4
98	A Simple Approach to Prepare Carboxycellulose Nanofibers from Untreated Biomass. Biomacromolecules, 2017, 18, 2333-2342.	2.6	124
99	Thin-film nanofibrous composite reverse osmosis membranes for desalination. Desalination, 2017, 420, 91-98.	4.0	69
100	Continuous fabrication of cellulose nanocrystal/poly(ethylene glycol) diacrylate hydrogel fiber from nanocomposite dispersion: Rheology, preparation and characterization. Polymer, 2017, 123, 55-64.	1.8	44
101	Fabrication of cellulose nanofiberâ€based ultrafiltration membranes by spray coating approach. Journal of Applied Polymer Science, 2017, 134, .	1.3	20
102	High performance thin-film nanofibrous composite hemodialysis membranes with efficient middle-molecule uremic toxin removal. Journal of Membrane Science, 2017, 523, 173-184.	4.1	111
103	Super-hydrophobic polyurethane sponges for oil absorption. Separation Science and Technology, 2017, 52, 221-227.	1.3	24
104	DEPENDENCE OF THE ONSET OF STRAIN-INDUCED CRYSTALLIZATION OF NATURAL RUBBER AND ITS SYNTHETIC ANALOGUE ON CROSSLINK AND ENTANGLEMENT BY USING SYNCHROTRON X-RAY. Rubber Chemistry and Technology, 2017, 90, 728-742.	0.6	14
105	The supramolecular structure of bone: X-ray scattering analysis and lateral structure modeling. Acta Crystallographica Section D: Structural Biology, 2016, 72, 986-996.	1.1	5
106	Electrospun nanofiber membranes. Current Opinion in Chemical Engineering, 2016, 12, 62-81.	3.8	200
107	Super-Robust Polylactide Barrier Films by Building Densely Oriented Lamellae Incorporated with Ductile in Situ Nanofibrils of Poly(butylene adipate- <i>co</i> -terephthalate). ACS Applied Materials & Interfaces, 2016, 8, 8096-8109.	4.0	102
108	In Situ Nanofibrillar Networks Composed of Densely Oriented Polylactide Crystals as Efficient Reinforcement and Promising Barrier Wall for Fully Biodegradable Poly(butylene succinate) Composite Films. ACS Sustainable Chemistry and Engineering, 2016, 4, 2887-2897.	3.2	43

#	Article	IF	CITATIONS
109	Low pressure UV-cured CS–PEO–PTEGDMA/PAN thin film nanofibrous composite nanofiltration membranes for anionic dye separation. Journal of Materials Chemistry A, 2016, 4, 15575-15588.	5.2	62
110	Large Scale Production of Continuous Hydrogel Fibers with Anisotropic Swelling Behavior by Dynamicâ€Crosslinkingâ€5pinning. Macromolecular Rapid Communications, 2016, 37, 1795-1801.	2.0	33
111	Nanoparticle–Nanofibrous Membranes as Scaffolds for Flexible Sweat Sensors. ACS Sensors, 2016, 1, 1060-1069.	4.0	28
112	Improvement of meltdown temperature of lithium-ion battery separator using electrospun polyethersulfone membranes. Polymer, 2016, 107, 163-169.	1.8	36
113	Biomimetic Nanofibrillation in Two-Component Biopolymer Blends with Structural Analogs to Spider Silk. Scientific Reports, 2016, 6, 34572.	1.6	24
114	Electrospun polystyrene nanofibrous membranes for direct contact membrane distillation. Journal of Membrane Science, 2016, 515, 86-97.	4.1	114
115	Polymeric nanostructured materials for biomedical applications. Progress in Polymer Science, 2016, 60, 86-128.	11.8	257
116	Probing structure and orientation in polymers using synchrotron small- and wide-angle X-ray scattering techniques. European Polymer Journal, 2016, 81, 433-446.	2.6	15
117	Deformation behavior of oriented β-crystals in injection-molded isotactic polypropylene by in situ X-ray scattering. Polymer, 2016, 84, 254-266.	1.8	22
118	High filtration performance thin film nanofibrous composite membrane prepared by electrospraying technique and hot-pressing treatment. Journal of Membrane Science, 2016, 499, 470-479.	4.1	49
119	Ultrafine Nanofibers. , 2016, , 1951-1953.		0
120	Self-Bundling Electrospinning Method. , 2016, , 1762-1763.		0
121	Insight into unique deformation behavior of oriented isotactic polypropylene with branched shish-kebabs. Polymer, 2015, 60, 274-283.	1.8	35
122	Thiol-functionalized chitin nanofibers for As (III) adsorption. Polymer, 2015, 60, 9-17.	1.8	69
123	Morphological and property investigations of carboxylated cellulose nanofibers extracted from different biological species. Cellulose, 2015, 22, 3127-3135.	2.4	20
124	Shear-Induced Precursor Relaxation-Dependent Growth Dynamics and Lamellar Orientation of β-Crystals in β-Nucleated Isotactic Polypropylene. Journal of Physical Chemistry B, 2015, 119, 5716-5727.	1.2	43
125	Micro-nano structure nanofibrous p-sulfonatocalix[8]arene complex membranes for highly efficient and selective adsorption of lanthanum( <scp>iii</scp> ) ions in aqueous solution. RSC Advances, 2015, 5, 21178-21188.	1.7	30
126	Structure and permeability relationships in polymer nanocomposites containing carbon black and organoclay. Polymer, 2015, 64, 19-28.	1.8	17

#	Article	IF	CITATIONS
127	Exploring the Nature of Cellulose Microfibrils. Biomacromolecules, 2015, 16, 1201-1209.	2.6	48
128	From Nanofibrillar to Nanolaminar Poly(butylene succinate): Paving the Way to Robust Barrier and Mechanical Properties for Full-Biodegradable Poly(lactic acid) Films. ACS Applied Materials & Interfaces, 2015, 7, 8023-8032.	4.0	67
129	High-performance nanofibrous membrane for removal of Cr(VI) from contaminated water. Journal of Plastic Film and Sheeting, 2015, 31, 379-400.	1.3	25
130	Role of Stably Entangled Chain Network Density in Shish-Kebab Formation in Polyethylene under an Intense Flow Field. Macromolecules, 2015, 48, 6652-6661.	2.2	57
131	Modified Cellulose. , 2015, , 1-2.		3
132	Electrospun Nanofibrous Membranes for Liquid Filtration. Nanostructure Science and Technology, 2014, , 325-354.	0.1	3
133	Characterization of TEMPO-oxidized cellulose nanofibers in aqueous suspension by small-angle X-ray scattering. Journal of Applied Crystallography, 2014, 47, 788-798.	1.9	49
134	Functionalized electrospun nanofibrous microfiltration membranes for removal of bacteria and viruses. Journal of Membrane Science, 2014, 452, 446-452.	4.1	142
135	Improving toughness of ultra-high molecular weight polyethylene with ionic liquid modified carbon nanofiber. Polymer, 2014, 55, 160-165.	1.8	17
136	Carbon nanotube surface-induced crystallization of polyethylene terephthalate (PET). Polymer, 2014, 55, 642-650.	1.8	36
137	Low-dimensional carbonaceous nanofiller induced polymer crystallization. Progress in Polymer Science, 2014, 39, 555-593.	11.8	140
138	A novel way to monitor the sequential destruction of parent-daughter crystals in isotactic polypropylene under uniaxial tension. Journal of Materials Science, 2014, 49, 3016-3024.	1.7	15
139	Nanofibrous polydopamine complex membranes for adsorption of Lanthanum (III) ions. Chemical Engineering Journal, 2014, 244, 307-316.	6.6	106
140	Nanofiltration membranes prepared by interfacial polymerization on thin-film nanofibrous composite scaffold. Polymer, 2014, 55, 1358-1366.	1.8	109
141	Nanofibrous ultrafiltration membranes containing cross-linked poly(ethylene glycol) and cellulose nanofiber composite barrier layer. Polymer, 2014, 55, 366-372.	1.8	80
142	Thiol-modified cellulose nanofibrous composite membranes for chromium (VI) and lead (II) adsorption. Polymer, 2014, 55, 1167-1176.	1.8	211
143	Simultaneous improvement of strength and toughness in fiber reinforced isotactic polypropylene composites by shear flow and a β-nucleating agent. RSC Advances, 2014, 4, 14766-14776.	1.7	38
144	Effects of molecular geometry on the self-assembly of giant polymer–dendron conjugates in condensed state. Soft Matter, 2014, 10, 3200.	1.2	12

#	Article	IF	CITATIONS
145	Self-reinforced polyethylene blend for artificial joint application. Journal of Materials Chemistry B, 2014, 2, 971.	2.9	35
146	Unprecedented Access to Strong and Ductile Poly(lactic acid) by Introducing In Situ Nanofibrillar Poly(butylene succinate) for Green Packaging. Biomacromolecules, 2014, 15, 4054-4064.	2.6	149
147	Strong and tough micro/nanostructured poly(lactic acid) by mimicking the multifunctional hierarchy of shell. Materials Horizons, 2014, 1, 546-552.	6.4	61
148	Dual-Biomimetic Superhydrophobic Electrospun Polystyrene Nanofibrous Membranes for Membrane Distillation. ACS Applied Materials & Interfaces, 2014, 6, 2423-2430.	4.0	141
149	Nanofiltration membranes based on thin-film nanofibrous composites. Journal of Membrane Science, 2014, 469, 188-197.	4.1	80
150	Fabrication and characterization of cellulose nanofiber based thin-film nanofibrous composite membranes. Journal of Membrane Science, 2014, 454, 272-282.	4.1	150
151	Improved barrier properties of poly(lactic acid) with randomly dispersed graphene oxide nanosheets. Journal of Membrane Science, 2014, 464, 110-118.	4.1	170
152	Benzyl-Modified Cellulose. , 2014, , 1-2.		0
153	Nanofibrous microfiltration membranes capable of removing bacteria, viruses and heavy metal ions. Journal of Membrane Science, 2013, 446, 376-382.	4.1	215
154	High-pressure crystallization of poly(lactic acid) with and without N2 atmosphere protection. Journal of Materials Science, 2013, 48, 7374-7383.	1.7	5
155	High flux ethanol dehydration using nanofibrous membranes containing graphene oxide barrier layers. Journal of Materials Chemistry A, 2013, 1, 12998.	5.2	84
156	Control of structure and morphology of highly aligned PLLA ultrafine fibers via linear-jet electrospinning. Polymer, 2013, 54, 6045-6051.	1.8	28
157	Strong Shear Flow-Driven Simultaneous Formation of Classic Shish-Kebab, Hybrid Shish-Kebab, and Transcrystallinity in Poly(lactic acid)/Natural Fiber Biocomposites. ACS Sustainable Chemistry and Engineering, 2013, 1, 1619-1629.	3.2	89
158	Structure Evolution upon Uniaxial Drawing Skin―and Coreâ€Layers of Injectionâ€Molded Isotactic Polypropylene by <i>In Situ</i> Synchrotron Xâ€ray Scattering. Journal of Polymer Science, Part B: Polymer Physics, 2013, 51, 1618-1631.	2.4	12
159	2D WAXS/SAXS study on isotactic propylene-1-butylene random copolymer subjected to uniaxial stretching: The influence of temperature. Polymer, 2013, 54, 1432-1439.	1.8	42
160	The effect of comonomer content on structure and property relationship of propylene-1-octene copolymer during uniaxial stretching. Polymer, 2013, 54, 4545-4554.	1.8	6
161	Effects of degumming conditions on electro-spinning rate of regenerated silk. International Journal of Biological Macromolecules, 2013, 61, 50-57.	3.6	32
162	High-flux microfiltration filters based on electrospun polyvinylalcohol nanofibrous membranes. Polymer, 2013, 54, 548-556.	1.8	128

#	Article	IF	CITATIONS
163	High flux low pressure thin film nanocomposite ultrafiltration membranes based on nanofibrous substrates. Separation and Purification Technology, 2013, 108, 143-151.	3.9	70
164	Crystal and Crystallites Structure of Natural Rubber and Synthetic <i>cis</i> -1,4-Polyisoprene by a New Two Dimensional Wide Angle X-ray Diffraction Simulation Method. I. Strain-Induced Crystallization. Macromolecules, 2013, 46, 4520-4528.	2.2	59
165	Crystalline Structure Changes in Preoriented Metallocene-Based Isotactic Polypropylene upon Annealing. Journal of Physical Chemistry B, 2013, 117, 7113-7122.	1.2	17
166	Plastic Deformation of Semicrystalline Polyethylene by X-ray Scattering: Comparison with Atomistic Simulations. Macromolecules, 2013, 46, 5279-5289.	2.2	38
167	Flow-induced crystallization precursor structure in high molecular weight isotactic polypropylene (HMW-iPP)/low molecular weight linear low density polyethylene (LMW-LLDPE) binary blends. Polymer, 2013, 54, 1425-1431.	1.8	15
168	Entanglements and Networks to Strain-Induced Crystallization and Stress–Strain Relations in Natural Rubber and Synthetic Polyisoprene at Various Temperatures. Macromolecules, 2013, 46, 5238-5248.	2.2	132
169	Crystal and Crystallites Structure of Natural Rubber and Peroxide-Vulcanized Natural Rubber by a Two-Dimensional Wide-Angle X-ray Diffraction Simulation Method. II. Strain-Induced Crystallization versus Temperature-Induced Crystallization. Macromolecules, 2013, 46, 9712-9721.	2.2	45
170	Morphology and mechanical properties of heterophasic PP–EP/EVA/organoclay nanocomposites. Journal of Applied Polymer Science, 2013, 128, 3473-3479.	1.3	6
171	Self-Bundling Electrospinning Method. , 2013, , 1-2.		0
172	Nanoclays. , 2013, , 1-2.		0
173	Polymeric nanofibrous composite membranes for energy efficient ethanol dehydration. Journal of Renewable and Sustainable Energy, 2012, 4, .	0.8	10
174	Structure Development during Stretching and Heating of Isotactic Propylene–1-Butylene Random Copolymer: From Unit Cells to Lamellae. Macromolecules, 2012, 45, 7061-7071.	2.2	24
175	Formation of Shish-Kebabs in Injection-Molded Poly( <scp>l</scp> -lactic acid) by Application of an Intense Flow Field. ACS Applied Materials & amp; Interfaces, 2012, 4, 6774-6784.	4.0	128
176	Nanofibrous Microfiltration Membrane Based on Cellulose Nanowhiskers. Biomacromolecules, 2012, 13, 180-186.	2.6	201
177	Tuning the Superstructure of Ultrahigh-Molecular-Weight Polyethylene/Low-Molecular-Weight Polyethylene Blend for Artificial Joint Application. ACS Applied Materials & Interfaces, 2012, 4, 1521-1529.	4.0	66
178	Suppressing of γ-Crystal Formation in Metallocene-Based Isotactic Polypropylene during Isothermal Crystallization under Shear Flow. Journal of Physical Chemistry B, 2012, 116, 5056-5063.	1.2	17
179	Phase Transitions in Prequenched Mesomorphic Isotactic Polypropylene during Heating and Annealing Processes As Revealed by Simultaneous Synchrotron SAXS and WAXD Technique. Journal of Physical Chemistry B, 2012, 116, 147-153.	1.2	37
180	Design and Synthesis of Network-Forming Triblock Copolymers Using Tapered Block Interfaces. ACS Macro Letters, 2012, 1, 519-523.	2.3	38

#	Article	IF	CITATIONS
181	Tough and Elastic Thermoplastic Organogels and Elastomers Made of Semicrystalline Polyolefin-Based Block Copolymers. Macromolecules, 2012, 45, 5604-5618.	2.2	41
182	The effects of endlinking network and entanglement to stress–strain relation and strain-induced crystallization of un-vulcanized and vulcanized natural rubber. Polymer, 2012, 53, 3325-3330.	1.8	76
183	Micro-nano structure poly(ether sulfones)/poly(ethyleneimine) nanofibrous affinity membranes for adsorption of anionic dyes and heavy metal ions in aqueous solution. Chemical Engineering Journal, 2012, 197, 88-100.	6.6	250
184	Highly Permeable Polymer Membranes Containing Directed Channels for Water Purification. ACS Macro Letters, 2012, 1, 723-726.	2.3	154
185	Chain Dynamics and Strain-Induced Crystallization of Pre- and Postvulcanized Natural Rubber Latex Using Proton Multiple Quantum NMR and Uniaxial Deformation by <i>in Situ</i> Synchrotron X-ray Diffraction. Macromolecules, 2012, 45, 6491-6503.	2.2	36
186	Shear Flow and Carbon Nanotubes Synergistically Induced Nonisothermal Crystallization of Poly(lactic acid) and Its Application in Injection Molding. Biomacromolecules, 2012, 13, 3858-3867.	2.6	95
187	Ultrafine Cellulose Nanofibers as Efficient Adsorbents for Removal of UO <sub>2</sub> <sup>2+</sup> in Water. ACS Macro Letters, 2012, 1, 213-216.	2.3	187
188	Inducing Order from Disordered Copolymers: On Demand Generation of Triblock Morphologies Including Networks. Macromolecules, 2012, 45, 4599-4605.	2.2	16
189	Time-Resolved Synchrotron X-ray Scattering Study on Propylene–1-Butylene Random Copolymer Subjected to Uniaxial Stretching at High Temperatures. Macromolecules, 2012, 45, 951-961.	2.2	32
190	Strainâ€induced crystallization and mechanical properties of functionalized graphene sheetâ€filled natural rubber. Journal of Polymer Science, Part B: Polymer Physics, 2012, 50, 718-723.	2.4	94
191	Microstructure and mechanical properties of isotactic polypropylene composite with twoâ€scale reinforcement. Polymers for Advanced Technologies, 2012, 23, 1580-1589.	1.6	10
192	Easy alignment and effective nucleation activity of ramie fibers in injectionâ€molded poly(lactic acid) biocomposites. Biopolymers, 2012, 97, 825-839.	1.2	60
193	Electrospun nanofibrous membranes for high flux microfiltration. Journal of Membrane Science, 2012, 392-393, 167-174.	4.1	253
194	Low pressure high flux thin film nanofibrous composite membranes prepared by electrospraying technique combined with solution treatment. Journal of Membrane Science, 2012, 394-395, 241-247.	4.1	61
195	Novel nanofibrous scaffolds for water filtration with bacteria and virus removal capability. Journal of Electron Microscopy, 2011, 60, 201-209.	0.9	90
196	Wide-Angle X-ray Scattering Study on Shear-Induced Crystallization of Propylene-1-Butylene Random Copolymer: Experiment and Diffraction Pattern Simulation. Macromolecules, 2011, 44, 558-565.	2.2	28
197	Real-Time Structure Changes during Uniaxial Stretching of Poly(ω-pentadecalactone) by <i>in Situ</i> Synchrotron WAXD/SAXS Techniques. Macromolecules, 2011, 44, 3874-3883.	2.2	46
198	In Situ Synchrotron X-ray Scattering Study on Isotactic Polypropylene Crystallization under the Coexistence of Shear Flow and Carbon Nanotubes. Macromolecules, 2011, 44, 8080-8092.	2.2	89

#	Article	IF	CITATIONS
199	Graphene Nanosheets and Shear Flow Induced Crystallization in Isotactic Polypropylene Nanocomposites. Macromolecules, 2011, 44, 2808-2818.	2.2	160
200	Suppressing the Skin–Core Structure of Injection-Molded Isotactic Polypropylene via Combination of an in situ Microfibrillar Network and an Interfacial Compatibilizer. Journal of Physical Chemistry B, 2011, 115, 7497-7504.	1.2	44
201	Effects of Block Architecture on Structure and Mechanical Properties of Olefin Block Copolymers under Uniaxial Deformation. Macromolecules, 2011, 44, 3670-3673.	2.2	55
202	Deformation-Induced Structure Changes in Elastomeric Nanocomposites. Advanced Structured Materials, 2011, , 135-154.	0.3	2
203	Ultrafine Polysaccharide Nanofibrous Membranes for Water Purification. Biomacromolecules, 2011, 12, 970-976.	2.6	212
204	Ultra-fine cellulose nanofibers: new nano-scale materials for water purification. Journal of Materials Chemistry, 2011, 21, 7507.	6.7	250
205	An in-situ X-ray scattering study during uniaxial stretching of ionic liquid/ultra-high molecular weight polyethylene blends. Polymer, 2011, 52, 4610-4618.	1.8	30
206	Poly(ethyleneimine) nanofibrous affinity membrane fabricated via one step wet-electrospinning from poly(vinyl alcohol)-doped poly(ethyleneimine) solution system and its application. Journal of Membrane Science, 2011, 379, 191-199.	4.1	93
207	Development of internal fine structure in stretched rubber vulcanizates. Journal of Polymer Science, Part B: Polymer Physics, 2011, 49, 1157-1162.	2.4	5
208	Rupture, orientation and strain-induced crystallization of polymer chain and network in vulcanized polyisoprene during uniaxial deformation by in-situ Electron Spin Resonance (ESR) and synchrotron X-ray analysis. Polymer, 2011, 52, 2453-2459.	1.8	18
209	Thin-film nanofibrous composite membranes containing cellulose or chitin barrier layers fabricated by ionic liquids. Polymer, 2011, 52, 2594-2599.	1.8	84
210	Fabrication of Micro-Nano Structure Nanofibers by Solvent Etching. Journal of Nanoscience and Nanotechnology, 2011, 11, 6919-6925.	0.9	10
211	Debranching and crystallization of waxy maize starch in relation to enzyme digestibility. Carbohydrate Polymers, 2010, 81, 385-393.	5.1	99
212	Fabrication of thin-film nanofibrous composite membranes by interfacial polymerization using ionic liquids as additives. Journal of Membrane Science, 2010, 365, 52-58.	4.1	98
213	Development of hydrophilic barrier layer on nanofibrous substrate as composite membrane via a facile route. Journal of Membrane Science, 2010, 356, 110-116.	4.1	111
214	Effects of molecular weight on poly(ω-pentadecalactone) mechanical and thermal properties. Polymer, 2010, 51, 1088-1099.	1.8	67
215	Characterization of nanoclay orientation in polymer nanocomposite film by small-angle X-ray scattering. Polymer, 2010, 51, 5255-5266.	1.8	31
216	Crystallization behavior of isotactic propyleneâ€lâ€hexene random copolymer revealed by timeâ€resolved SAXS/WAXD techniques. Journal of Polymer Science, Part B: Polymer Physics, 2010, 48, 26-32.	2.4	11

#	Article	IF	CITATIONS
217	Processingâ€structureâ€mechanical property relationships of semicrystalline polyolefinâ€based block copolymers. Journal of Polymer Science, Part B: Polymer Physics, 2010, 48, 1428-1437.	2.4	38
218	Aligned and molecularly oriented semihollow ultrafine polymer fiber yarns by a facile method. Journal of Polymer Science, Part B: Polymer Physics, 2010, 48, 1118-1125.	2.4	25
219	Molecular orientation and stress relaxation during strain-induced crystallization of vulcanized natural rubber. Polymer Journal, 2010, 42, 474-481.	1.3	46
220	Shear Enhanced Crystallization and Tensile Behaviors of Oscillation Shear Injection Molded Poly(ethylene terephthalate). Journal of Macromolecular Science - Physics, 2010, 50, 383-397.	0.4	5
221	Thin-Film Nanofibrous Composite Ultrafiltration Membranes Based on Polyvinyl Alcohol Barrier Layer Containing Directional Water Channels. Industrial & Engineering Chemistry Research, 2010, 49, 11978-11984.	1.8	47
222	Isothermal Crystallization of Poly( <scp>l</scp> -lactide) Induced by Graphene Nanosheets and Carbon Nanotubes: A Comparative Study. Macromolecules, 2010, 43, 5000-5008.	2.2	308
223	An <i>in Situ</i> X-ray Structural Study of Olefin Block and Random Copolymers under Uniaxial Deformation. Macromolecules, 2010, 43, 1922-1929.	2.2	73
224	Spatial Distribution of γ-Crystals in Metallocene-Made Isotactic Polypropylene Crystallized under Combined Thermal and Flow Fields. Journal of Physical Chemistry B, 2010, 114, 6806-6816.	1.2	25
225	Molecular dynamics of natural rubber as revealed by dielectric spectroscopy: The role of natural cross–linking. Soft Matter, 2010, 6, 3636.	1.2	47
226	Step-Cycle Mechanical Processing of Gels of sPP- <i>b</i> -EPR- <i>b</i> -sPP Triblock Copolymer in Mineral Oil. Macromolecules, 2010, 43, 6782-6788.	2.2	37
227	Competitive Growth of α- and β-Crystals in β-Nucleated Isotactic Polypropylene under Shear Flow. Macromolecules, 2010, 43, 6760-6771.	2.2	128
228	Phase Behavior of Neat Triblock Copolymers and Copolymer/Homopolymer Blends Near Network Phase Windows. Macromolecules, 2010, 43, 9039-9048.	2.2	32
229	Preferred Orientation in Polymer Fiber Scattering. Polymer Reviews, 2010, 50, 91-111.	5.3	42
230	High-flux thin-film nanofibrous composite ultrafiltration membranes containing cellulose barrier layer. Journal of Materials Chemistry, 2010, 20, 4692.	6.7	125
231	A Springâ€Like Behavior of Chiral Block Copolymer with Helical Nanostructure Driven by Crystallization. Advanced Functional Materials, 2009, 19, 448-459.	7.8	31
232	The role of multi-walled carbon nanotubes in shear enhanced crystallization of isotactic poly(1-butene). Journal of Thermal Analysis and Calorimetry, 2009, 98, 611-622.	2.0	21
233	Polypentadecalactone prepared by lipase catalysis: crystallization kinetics and morphology. Polymer International, 2009, 58, 944-953.	1.6	31
234	Design and fabrication of electrospun polyethersulfone nanofibrous scaffold for highâ€flux nanofiltration membranes. Journal of Polymer Science, Part B: Polymer Physics, 2009, 47, 2288-2300.	2.4	84

**BENJAMIN S HSIAO** 

#	Article	IF	CITATIONS
235	The role of polymers in breakthrough technologies for water purification. Journal of Polymer Science, Part B: Polymer Physics, 2009, 47, 2431-2435.	2.4	45
236	High flux nanofiltration membranes based on interfacially polymerized polyamide barrier layer on polyacrylonitrile nanofibrous scaffolds. Journal of Membrane Science, 2009, 326, 484-492.	4.1	237
237	UV-cured poly(vinyl alcohol) ultrafiltration nanofibrous membrane based on electrospun nanofiber scaffolds. Journal of Membrane Science, 2009, 328, 1-5.	4.1	91
238	High flux ultrafiltration nanofibrous membranes based on polyacrylonitrile electrospun scaffolds and crosslinked polyvinyl alcohol coating. Journal of Membrane Science, 2009, 338, 145-152.	4.1	138
239	New insights into the relationship between network structure and strain-induced crystallization in un-vulcanized and vulcanized natural rubber by synchrotron X-ray diffraction. Polymer, 2009, 50, 2142-2148.	1.8	107
240	Formation of functional polyethersulfone electrospun membrane for water purification by mixed solvent and oxidation processes. Polymer, 2009, 50, 2893-2899.	1.8	156
241	Chemical crosslinking and biophysical properties of electrospun hyaluronic acid based ultra-thin fibrous membranes. Polymer, 2009, 50, 3762-3769.	1.8	59
242	Block Copolymers with a Twist. Journal of the American Chemical Society, 2009, 131, 18533-18542.	6.6	126
243	Influence of LC Content on the Phase Structures of Side-Chain Liquid Crystalline Block Copolymers with Bent-Core Mesogens. Macromolecules, 2009, 42, 3510-3517.	2.2	20
244	Small-angle X-ray scattering study of intramuscular fish bone: collagen fibril superstructure determined from equidistant meridional reflections. Journal of Applied Crystallography, 2008, 41, 252-261.	1.9	31
245	Multiâ€scaled microstructures in natural rubber characterized by synchrotron Xâ€ray scattering and optical microscopy. Journal of Polymer Science, Part B: Polymer Physics, 2008, 46, 2456-2464.	2.4	59
246	Enhanced Mechanical Performance of Selfâ€Bundled Electrospun Fiber Yarns via Postâ€Treatments. Macromolecular Rapid Communications, 2008, 29, 826-831.	2.0	87
247	Combined effect of shear and fibrous fillers on orientation-induced crystallization in discontinuous aramid fiber/isotactic polypropylene composites. Polymer, 2008, 49, 295-302.	1.8	56
248	The relationship between microstructure and toughness of biaxially oriented semicrystalline polyester films. Polymer, 2008, 49, 2507-2514.	1.8	46
249	Crystal Orientation Change and Its Origin in One-Dimensional Nanoconfinement Constructed by Polystyrene- <i>block</i> -poly(ethylene oxide) Single Crystal Mats. Macromolecules, 2008, 41, 8114-8123.	2.2	65
250	Lateral Packing of Mineral Crystals in Bone Collagen Fibrils. Biophysical Journal, 2008, 95, 1985-1992.	0.2	77
251	Effect of Nanoclay on Natural Rubber Microstructure. Macromolecules, 2008, 41, 6763-6772.	2.2	144
252	Continuous polymer nanofiber yarns prepared by self-bundling electrospinning method. Polymer, 2008, 49, 2755-2761.	1.8	150

#	Article	IF	CITATIONS
253	Functional nanofibers for environmental applications. Journal of Materials Chemistry, 2008, 18, 5326.	6.7	388
254	Competition between liquid crystallinity and block copolymerself-assembly in core–shell rod–coil block copolymers. Soft Matter, 2008, 4, 458-461.	1.2	32
255	Formation and Stability of Shear-Induced Shish-Kebab Structure in Highly Entangled Melts of UHMWPE/HDPE Blends. Macromolecules, 2008, 41, 4766-4776.	2.2	162
256	New Insights into Lamellar Structure Development and SAXS/WAXD Sequence Appearance during Uniaxial Stretching of Amorphous Poly(ethylene terephthalate) above Glass Transition Temperature. Macromolecules, 2008, 41, 2859-2867.	2.2	58
257	Real-Time Crystallization of Organoclay Nanoparticle Filled Natural Rubber under Stretching. Macromolecules, 2008, 41, 2295-2298.	2.2	61
258	Strain-Induced Crystallization of Natural Rubber: Effect of Proteins and Phospholipids. Rubber Chemistry and Technology, 2008, 81, 753-766.	0.6	88
259	Lamellar nanostructure in 'Somasif'-based organoclays. Clays and Clay Minerals, 2007, 55, 140-150.	0.6	20
260	Antithrombogenic property of bone marrow mesenchymal stem cells in nanofibrous vascular grafts. Proceedings of the National Academy of Sciences of the United States of America, 2007, 104, 11915-11920.	3.3	360
261	Structure Study of Cellulose Fibers Wet-Spun from Environmentally Friendly NaOH/Urea Aqueous Solutions. Biomacromolecules, 2007, 8, 1918-1926.	2.6	121
262	Surface Modification of Nanoclays by Catalytically Active Transition Metal Ions. Langmuir, 2007, 23, 9808-9815.	1.6	30
263	Stabilizing Thin Film Polymer Bilayers against Dewetting Using Multiwalled Carbon Nanotubes. Macromolecules, 2007, 40, 9510-9516.	2.2	29
264	Poly(ethylene oxide) Crystal Orientation Changes in an Inverse Hexagonal Cylindrical Phase Morphology Constructed by a Poly(ethylene oxide)-block-polystyrene Diblock Copolymer. Macromolecules, 2007, 40, 526-534.	2.2	36
265	Hierarchical Nanostructures of Bent-Core Molecules Blended with Poly(styrene-b-4-vinylpyridine) Block Copolymer. Macromolecules, 2007, 40, 5095-5102.	2.2	26
266	Side-Chain Liquid Crystalline Poly(meth)acrylates with Bent-Core Mesogens. Macromolecules, 2007, 40, 840-848.	2.2	39
267	Bioactive Nanofibers:Â Synergistic Effects of Nanotopography and Chemical Signaling on Cell Guidance. Nano Letters, 2007, 7, 2122-2128.	4.5	339
268	Morphological features and melting behavior of nanocomposites based on isotactic polypropylene and multiwalled carbon nanotubes. Journal of Applied Polymer Science, 2007, 106, 2640-2647.	1.3	46
269	Functionalization of poly(L-lactide) nanofibrous scaffolds with bioactive collagen molecules. Journal of Biomedical Materials Research - Part A, 2007, 83A, 1117-1127.	2.1	62
270	Role of stearic acid in the strain-induced crystallization of crosslinked natural rubber and synthetic cis-1,4-polyisoprene. Polymer, 2007, 48, 3801-3808.	1.8	46

#	Article	IF	CITATIONS
271	Acceleration or retardation to crystallization if liquid–liquid phase separation occurs: Studies on a polyolefin blend by SAXS/WAXD, DSC and TEM. Polymer, 2007, 48, 6668-6680.	1.8	27
272	The role of interlamellar chain entanglement in deformation-induced structure changes during uniaxial stretching of isotactic polypropylene. Polymer, 2007, 48, 6867-6880.	1.8	173
273	Deformation-induced highly oriented and stable mesomorphic phase in quenched isotactic polypropylene. Polymer, 2007, 48, 6934-6947.	1.8	47
274	Small-angle X-ray study of the three-dimensional collagen/mineral superstructure in intramuscular fish bone. Journal of Applied Crystallography, 2007, 40, s666-s668.	1.9	17
275	Functional electrospun nanofibrous scaffolds for biomedical applications. Advanced Drug Delivery Reviews, 2007, 59, 1392-1412.	6.6	861
276	Polymer nanocomposites based on transition metal ion modified organoclays. Polymer, 2007, 48, 827-840.	1.8	24
277	Probing nucleation and growth behavior of twisted kebabs from shish scaffold in sheared polyethylene melts by in situ X-ray studies. Polymer, 2007, 48, 4511-4519.	1.8	59
278	Role of Chain Entanglement Network on Formation of Flow-Induced Crystallization Precursor Structure. , 2007, , 133-149.		7
279	Shearâ€Induced Orientation and Structure Development in Isotactic Polypropylene Melt Containing Modified Carbon Nanofibers. Journal of Macromolecular Science - Physics, 2006, 45, 247-261.	0.4	31
280	Myotube Assembly on Nanofibrous and Micropatterned Polymers. Nano Letters, 2006, 6, 537-542.	4.5	293
281	Patterning Polyethylene Oligomers on Carbon Nanotubes Using Physical Vapor Deposition. Nano Letters, 2006, 6, 1007-1012.	4.5	126
282	NANOFIBROUS MATERIALS AND THEIR APPLICATIONS. Annual Review of Materials Research, 2006, 36, 333-368.	4.3	573
283	Thermal Stability of Shear-Induced Shish-Kebab Precursor Structure from High Molecular Weight Polyethylene Chains. Macromolecules, 2006, 39, 2209-2218.	2.2	102
284	Trilayer Crystalline Lamellar Morphology under Confinement. Macromolecules, 2006, 39, 2739-2742.	2.2	21
285	Structure Evolution during Cyclic Deformation of an Elastic Propylene-Based Ethyleneâ^Propylene Copolymer. Macromolecules, 2006, 39, 3588-3597.	2.2	62
286	Lamellar Formation and Relaxation in Simple Sheared Poly(ethylene terephthalate) by Small-Angle X-ray Scattering. Macromolecules, 2006, 39, 2930-2939.	2.2	40
287	Crystallization and Stress Relaxation in Highly Stretched Samples of Natural Rubber and Its Synthetic Analogue. Macromolecules, 2006, 39, 5100-5105.	2.2	95
288	In-Situ X-ray Deformation Study of Fluorinated Multiwalled Carbon Nanotube and Fluorinated Ethyleneâ^'Propylene Nanocomposite Fibers. Macromolecules, 2006, 39, 5427-5437.	2.2	40

#	Article	IF	CITATIONS
289	Superstructure Evolution in Poly(ethylene terephthalate) during Uniaxial Deformation above Glass Transition Temperature. Macromolecules, 2006, 39, 2909-2920.	2.2	61
290	Development of Multiple-Jet Electrospinning Technology. ACS Symposium Series, 2006, , 91-105.	0.5	12
291	Probing the flow-induced shish-kebab structure in entangled polyethylene melts by synchrotron X-ray scattering. Journal of Applied Crystallography, 2006, 40, s48-s51.	1.9	7
292	Thermal stability of shear-induced precursor structures in isotactic polypropylene by rheo-X-ray techniques with couette flow geometry. Journal of Polymer Science, Part B: Polymer Physics, 2006, 44, 3553-3570.	2.4	30
293	Comparison of poly(ethylene oxide) crystal orientations and crystallization behaviors in nano-confined cylinders constructed by a poly(ethylene oxide)-b-polystyrene diblock copolymer and a blend of poly(ethylene oxide)-b-polystyrene and polystyrene. Polymer, 2006, 47, 5457-5466.	1.8	87
294	High flux ultrafiltration membranes based on electrospun nanofibrous PAN scaffolds and chitosan coating. Polymer, 2006, 47, 2434-2441.	1.8	503
295	In situ WAXD study of structure changes during uniaxial deformation of ethylene-based semicrystalline ethylene–propylene copolymer. Polymer, 2006, 47, 2884-2893.	1.8	28
296	Relationship between structure and dynamic mechanical properties of a carbon nanofiber reinforced elastomeric nanocomposite. Polymer, 2006, 47, 6797-6807.	1.8	17
297	High performance ultrafiltration composite membranes based on poly(vinyl alcohol) hydrogel coating on crosslinked nanofibrous poly(vinyl alcohol) scaffold. Journal of Membrane Science, 2006, 278, 261-268.	4.1	225
298	Effects of high molecular weight species on shear-induced orientation and crystallization of isotactic polypropylene. Polymer, 2006, 47, 5657-5668.	1.8	89
299	X-ray studies of regenerated cellulose fibers wet spun from cotton linter pulp in NaOH/thiourea aqueous solutions. Polymer, 2006, 47, 2839-2848.	1.8	107
300	Mineralization of hydroxyapatite in electrospun nanofibrous poly(L-lactic acid) scaffolds. Journal of Biomedical Materials Research - Part A, 2006, 79A, 307-317.	2.1	220
301	Electrospinning of Hyaluronic Acid (HA) and HA/Gelatin Blends. Macromolecular Rapid Communications, 2006, 27, 114-120.	2.0	134
302	The role of high molecular weight chains in flow-induced crystallization precursor structures. Journal of Physics Condensed Matter, 2006, 18, S2421-S2436.	0.7	12
303	Synchrotron X-Ray Studies of Vulcanized Rubbers and Thermoplastic Elastomers. Rubber Chemistry and Technology, 2006, 79, 460-488.	0.6	21
304	A new pathway for developingin vitronanostructured non-viral gene carriers. Journal of Physics Condensed Matter, 2006, 18, S2513-S2525.	0.7	11
305	Electrospun Nanofibrous Scaffolds for Biomedical Applications. Journal of Biomedical Nanotechnology, 2005, 1, 115-132.	0.5	44
306	Structural and morphological development in poly(ethylene-co-hexene) and poly(ethylene-co-butylene) blends due to the competition between liquid–liquid phase separation and crystallization. Polymer, 2005, 46, 2675-2684.	1.8	26

#	Article	IF	CITATIONS
307	Shear-induced crystallization in isotactic polypropylene containing ultra-high molecular weight polyethylene oriented precursor domains. Polymer, 2005, 46, 3096-3104.	1.8	62
308	Formation of water-resistant hyaluronic acid nanofibers by blowing-assisted electro-spinning and non-toxic post treatments. Polymer, 2005, 46, 4853-4867.	1.8	136
309	Uniaxial deformation of an elastomer nanocomposite containing modified carbon nanofibers by in situ synchrotron X-ray diffraction. Polymer, 2005, 46, 5103-5117.	1.8	45
310	Shear-induced crystallization of isotactic polypropylene within the oriented scaffold of noncrystalline ultrahigh molecular weight polyethylene. Polymer, 2005, 46, 8859-8871.	1.8	62
311	Flow-induced shish-kebab precursor structures in entangled polymer melts. Polymer, 2005, 46, 8587-8623.	1.8	427
312	Rheological study of carbon nanofiber induced physical gelation in polyolefin nanocomposite melt. Polymer, 2005, 46, 11591-11599.	1.8	55
313	Orientated crystallization in discontinuous aramid fiber/isotactic polypropylene composites under shear flow conditions. Journal of Applied Polymer Science, 2005, 98, 1113-1118.	1.3	20
314	In Vitro Mineralization of Collagen in Demineralized Fish Bone. Macromolecular Chemistry and Physics, 2005, 206, 43-51.	1.1	43
315	Crystallization of Polystyrene-block-[Syndiotactic Poly(propylene)] Block Copolymers from Confinement to Breakout. Macromolecular Rapid Communications, 2005, 26, 107-111.	2.0	33
316	Electrospun fine-textured scaffolds for heart tissue constructs. Biomaterials, 2005, 26, 5330-5338.	5.7	597
317	Unexpected Shish-Kebab Structure in a Sheared Polyethylene Melt. Physical Review Letters, 2005, 94, 117802.	2.9	254
318	In vitro non-viral gene delivery with nanofibrous scaffolds. Nucleic Acids Research, 2005, 33, e170-e170.	6.5	102
319	Synchrotron X-ray scattering studies of the nature of shear-induced shish-kebab structure in polyethylene melt. , 2005, , 114-126.		6
320	Probing the Nature of Strain-Induced Crystallization in Polyisoprene Rubber by Combined Thermomechanical and In Situ X-ray Diffraction Techniques. Macromolecules, 2005, 38, 7064-7073.	2.2	85
321	Confined Discotic Liquid Crystalline Self-Assembly in a Novel Coilâ^'Coilâ^'Disk Triblock Oligomer. Macromolecules, 2005, 38, 3386-3394.	2.2	17
322	Chain-Folding and Overall Molecular Conformation in a Novel Amphiphilic Starlike Macromolecule. Macromolecules, 2005, 38, 7074-7082.	2.2	13
323	In-Situ X-ray Scattering Studies of a Unique Toughening Mechanism in Surface-Modified Carbon Nanofiber/UHMWPE Nanocomposite Films. Macromolecules, 2005, 38, 3883-3893.	2.2	70
324	Perforated Layer Structures in Liquid Crystalline Rodâ^'Coil Block Copolymers. Journal of the American Chemical Society, 2005, 127, 15481-15490.	6.6	124

**BENJAMIN S HSIAO** 

#	Article	IF	CITATIONS
325	Shear-Induced Molecular Orientation and Crystallization in Isotactic Polypropylene: Effects of the Deformation Rate and Strain. Macromolecules, 2005, 38, 1244-1255.	2.2	179
326	Deformation-Induced Phase Transition and Superstructure Formation in Poly(ethylene terephthalate). Macromolecules, 2005, 38, 91-103.	2.2	111
327	Probing Flow-Induced Precursor Structures in Blown Polyethylene Films by Synchrotron X-rays during Constrained Melting. Macromolecules, 2005, 38, 5128-5136.	2.2	29
328	Mechanism of strain-induced crystallization in filled and unfilled natural rubber vulcanizates. Journal of Applied Physics, 2005, 97, 103529.	1.1	140
329	High Flux Filtration Medium Based on Nanofibrous Substrate with Hydrophilic Nanocomposite Coating. Environmental Science & Technology, 2005, 39, 7684-7691.	4.6	348
330	Relationships between Structure and Rheology in Model Nanocomposites of Ethyleneâ^'Vinyl-Based Copolymers and Organoclays. Macromolecules, 2005, 38, 3765-3775.	2.2	60
331	Reversible De-Intercalation and Intercalation Induced by Polymer Crystallization and Melting in a Poly(ethylene oxide)/Organoclay Nanocomposite. Langmuir, 2005, 21, 5672-5676.	1.6	14
332	Strain-Induced Molecular Orientation and Crystallization in Natural and Synthetic Rubbers under Uniaxial Deformation by In-situ Synchrotron X-ray Study. Rubber Chemistry and Technology, 2004, 77, 317-335.	0.6	81
333	Prevention of Postsurgery-Induced Abdominal Adhesions by Electrospun Bioabsorbable Nanofibrous Poly(lactide-co-glycolide)-Based Membranes. Annals of Surgery, 2004, 240, 910-915.	2.1	178
334	Effect of Network-Chain Length on Strain-Induced Crystallization of NR and IR Vulcanizates. Rubber Chemistry and Technology, 2004, 77, 711-723.	0.6	89
335	Incorporation and controlled release of a hydrophilic antibiotic using poly(lactide-co-glycolide)-based electrospun nanofibrous scaffolds. Journal of Controlled Release, 2004, 98, 47-56.	4.8	707
336	In situ synchrotron SAXS/WAXD studies during melt spinning of modified carbon nanofiber and isotactic polypropylene nanocomposite. Colloid and Polymer Science, 2004, 282, 802-809.	1.0	19
337	Structural developments in synthetic rubbers during uniaxial deformation byin situ synchrotron X-ray diffraction. Journal of Polymer Science, Part B: Polymer Physics, 2004, 42, 956-964.	2.4	61
338	Anomalous rheology in a nanostructured diblock copolymer/hydrocarbon system and its kinetic origin. Journal of Polymer Science, Part B: Polymer Physics, 2004, 42, 1496-1505.	2.4	4
339	Pathway-Dependent Melting in a Low-Molecular-Weight Polyethylene-block-Poly(ethylene oxide) Diblock Copolymer. Macromolecular Rapid Communications, 2004, 25, 853-857.	2.0	30
340	Structural formation of amorphous poly(ethylene terephthalate) during uniaxial deformation above glass temperature. Polymer, 2004, 45, 905-918.	1.8	81
341	Comparison of crystallization kinetics in various nanoconfined geometries. Polymer, 2004, 45, 2931-2939.	1.8	76

 $_{342}$  Self-assembly and crystallization behavior of a double-crystalline polyethylene-block-poly(ethylene) Tj ETQq0 0 0 rg  $_{1.8}^{\text{PT}}$ /Overlock 10 Tf 50 rg  $_{1.8}^{\text{PT}}$ /Ov

#	Article	IF	CITATIONS
343	Shear-Induced Crystallization Precursor Studies in Model Polyethylene Blends by in-Situ Rheo-SAXS and Rheo-WAXD. Macromolecules, 2004, 37, 4845-4859.	2.2	197
344	Shear-Enhanced Crystallization in Isotactic Polypropylene. In-Situ Synchrotron SAXS and WAXD. Macromolecules, 2004, 37, 9005-9017.	2.2	132
345	Hierarchical Assembly of a Series of Rodâ^'Coil Block Copolymers:Â Supramolecular LC Phase in Nanoenviroment. Macromolecules, 2004, 37, 2854-2860.	2.2	97
346	Electro-Spinning and Electro-Blowing of Hyaluronic Acid. Biomacromolecules, 2004, 5, 1428-1436.	2.6	300
347	Ordering kinetics of body-centered-cubic morphology in diblock copolymer solutions at low temperatures. Journal of Rheology, 2004, 48, 1389-1405.	1.3	8
348	Orientation and Crystallization of Natural Rubber Network As Revealed by WAXD Using Synchrotron Radiation. Macromolecules, 2004, 37, 3299-3309.	2.2	273
349	Crystallization-Induced Undulated Morphology in Polystyrene-b-Poly(l-lactide) Block Copolymer. Macromolecules, 2004, 37, 5985-5994.	2.2	99
350	Confinement Size Effect on Crystal Orientation Changes of Poly(ethylene oxide) Blocks in Poly(ethylene oxide)-b-polystyrene Diblock Copolymers. Macromolecules, 2004, 37, 3689-3698.	2.2	130
351	Optimization and Characterization of Dextran Membranes Prepared by Electrospinning. Biomacromolecules, 2004, 5, 326-333.	2.6	253
352	Lattice Deformation of Strain-induced Crystallites in Carbon-filled Natural Rubber. Chemistry Letters, 2004, 33, 220-221.	0.7	18
353	Structure and Morphology Changes during in Vitro Degradation of Electrospun Poly(glycolide-co-lactide) Nanofiber Membrane. Biomacromolecules, 2003, 4, 416-423.	2.6	248
354	Synchrotron SAXS/WAXD and rheological studies of clay suspensions in silicone fluid. Journal of Colloid and Interface Science, 2003, 266, 339-345.	5.0	24
355	Control of degradation rate and hydrophilicity in electrospun non-woven poly(d,l-lactide) nanofiber scaffolds for biomedical applications. Biomaterials, 2003, 24, 4977-4985.	5.7	524
356	Physical gelation in ethylene–propylene copolymer melts induced by polyhedral oligomeric silsesquioxane (POSS) molecules. Polymer, 2003, 44, 1499-1506.	1.8	160
357	Molecular orientation and structural development in vulcanized polyisoprene rubbers during uniaxial deformation by in situ synchrotron X-ray diffraction. Polymer, 2003, 44, 6003-6011.	1.8	120
358	Effects of organoclays on morphology and thermal and rheological properties of polystyrene and poly(methyl methacrylate) blends. Journal of Polymer Science, Part B: Polymer Physics, 2003, 41, 44-54.	2.4	250
359	Crystallization and structure formation of poly(l-lactide-co-meso-lactide) random copolymers: a time-resolved wide- and small-angle X-ray scattering study. Polymer, 2003, 44, 711-717.	1.8	79
360	On the nature of multiple melting in poly(ethylene terephthalate) (PET) and its copolymers with cyclohexylene dimethylene terephthalate (PET/CT). Polymer, 2003, 44, 1527-1535.	1.8	64

#	Article	IF	CITATIONS
361	Structure and morphology development during deformation of propylene based ethylene–propylene copolymer and its blends with isotactic polypropylene. Polymer, 2003, 44, 2385-2392.	1.8	12
362	Control of structure, morphology and property in electrospun poly(glycolide-co-lactide) non-woven membranes via post-draw treatments. Polymer, 2003, 44, 4959-4967.	1.8	207
363	In situ observation of low molecular weight poly(ethylene oxide) crystal melting, recrystallization. Polymer, 2003, 44, 6051-6058.	1.8	41
364	Nature of Shear-Induced Primary Nuclei in iPP Melt. Journal of Macromolecular Science - Physics, 2003, 42, 515-531.	0.4	47
365	Shear-Induced Crystallization in Novel Long Chain Branched Polypropylenes by in Situ Rheo-SAXS and -WAXD. Macromolecules, 2003, 36, 5226-5235.	2.2	141
366	Mechanism of Structural Formation by Uniaxial Deformation in Amorphous Poly(ethylene) Tj ETQq0 0 0 rgBT /Ov	verlock 10	Tf <u>50</u> 542 Td
367	Nature of Strain-Induced Structures in Natural and Synthetic Rubbers under Stretching. Macromolecules, 2003, 36, 5915-5917.	2.2	104
368	Structure Changes during Uniaxial Deformation of Ethylene-Based Semicrystalline Ethyleneâ^'Propylene Copolymer. 1. SAXS Study. Macromolecules, 2003, 36, 1920-1929.	2.2	66
369	"Plastic Deformation―Mechanism and Phase Transformation in a Shear-Induced Metastable Hexagonally Perforated Layer Phase of a Polystyrene-b-poly(ethylene oxide) Diblock Copolymer. Macromolecules, 2003, 36, 3180-3188.	2.2	58
370	In-Situ Studies of Structure Development during Deformation of a Segmented Poly(urethaneâ^'urea) Elastomer. Macromolecules, 2003, 36, 1940-1954.	2.2	236
371	Uniaxial Deformation of Nylon 6–Clay Nanocomposites by In-Situ Synchrotron X-Ray Measurements. Journal of Macromolecular Science - Physics, 2003, 42, 201-214.	0.4	12
372	Combined techniques of Raman spectroscopy and synchrotron two-dimensional x-ray diffraction for situstudy of anisotropic system: Example of polymer fibers under deformation. Review of Scientific Instruments, 2003, 74, 3087-3092.	0.6	22
373	Crystallization and structure formation in polymer blends with strong intermodular interactions: blends of poly(ethylene oxide) and styrene-hydroxystyrene copolymers. Macromolecular Symposia, 2003, 198, 29-40.	0.4	2
374	Synchrotron Xâ€Ray scattering of polymer nanocomposites. Synchrotron Radiation News, 2002, 15, 20-34.	0.2	5
375	New Insights into Structural Development in Natural Rubber during Uniaxial Deformation by In Situ Synchrotron X-ray Diffraction. Macromolecules, 2002, 35, 6578-6584.	2.2	242
376	In-Situ Synchrotron WAXD/SAXS Studies of Structural Development during PBO/PPA Solution Spinning. Macromolecules, 2002, 35, 433-439.	2.2	35
377	Nanotailored Crystalline Morphology in Hexagonally Perforated Layers of a Self-Assembled PS-b-PEO Diblock Copolymer. Macromolecules, 2002, 35, 3553-3562.	2.2	90
378	A Synchrotron WAXD Study on the Early Stages of Coagulation during PBO Fiber Spinning. Macromolecules, 2002, 35, 9851-9853.	2.2	12

**BENJAMIN S HSIAO** 

#	Article	IF	CITATIONS
379	Salt-Induced Polymer Gelation and Formation of Nanocrystals in a Polymerâ^'Salt System. Langmuir, 2002, 18, 10402-10406.	1.6	10
380	Mesophase as the Precursor for Strain-Induced Crystallization in Amorphous Poly(ethylene) Tj ETQq0 0 0 rgBT /C	)verlock 10 2.2	0 T <u>f 5</u> 0 702 T 131
381	Nanostructure Evolution of Isotropic High-Pressure Injection-Molded UHMWPE during Heating. Macromolecules, 2002, 35, 2200-2206.	2.2	21
382	Shear-Enhanced Crystallization in Isotactic Polypropylene. 3. Evidence for a Kinetic Pathway to Nucleation. Macromolecules, 2002, 35, 1762-1769.	2.2	217
383	CHEMICAL APPLICATIONS OF SMALL ANGLE SCATTERING. Advanced Series in Physical Chemistry, 2002, , 799-849.	1.5	1
384	Phase Diagram of a Nearly Isorefractive Polyolefin Blend. Macromolecules, 2002, 35, 1072-1078.	2.2	79
385	Precursors of primary nucleation induced by flow in isotactic polypropylene. Physica A: Statistical Mechanics and Its Applications, 2002, 304, 145-157.	1.2	107
386	Manipulating the microstructure and rheology in polymer-organoclay composites. Polymer Engineering and Science, 2002, 42, 1841-1851.	1.5	29
387	Structure and process relationship of electrospun bioabsorbable nanofiber membranes. Polymer, 2002, 43, 4403-4412.	1.8	1,671
388	Structure development in the early stages of crystallization during melt spinning. Polymer, 2002, 43, 1873-1875.	1.8	54
389	Structure and property studies of bioabsorbable poly(glycolide-co-lactide) fiber during processing and in vitro degradation. Polymer, 2002, 43, 5527-5534.	1.8	48
390	Shear-Induced Precursor Structures in Isotactic Polypropylene Melt by in-Situ Rheo-SAXS and Rheo-WAXD Studies. Macromolecules, 2002, 35, 9096-9104.	2.2	219
391	Structure Development during Shear Flow Induced Crystallization of i-PP:Â In Situ Wide-Angle X-ray Diffraction Study. Macromolecules, 2001, 34, 5902-5909.	2.2	385
392	Small-Angle X-ray Scattering of Polymers. Chemical Reviews, 2001, 101, 1727-1762.	23.0	348
393	Initial-Stage Growth Controlled Crystal Orientations in Nanoconfined Lamellae of a Self-Assembled Crystallineâ <sup>~</sup> 'Amorphous Diblock Copolymer. Macromolecules, 2001, 34, 1244-1251.	2.2	152
394	Morphological Changes during the Annealing of Polybutene-1 Fiber. Macromolecules, 2001, 34, 2008-2011.	2.2	15
395	Structural and Morphological Studies of Isotactic Polypropylene Fibers during Heat/Draw Deformation by in-Situ Synchrotron SAXS/WAXD. Macromolecules, 2001, 34, 2569-2578.	2.2	172

396 Crystal Orientation Changes in Two-Dimensionally Confined Nanocylinders in a Poly(ethylene) Tj ETQq0 0 0 rgBT /Overlock 10 Tf 50 62

#	Article	IF	CITATIONS
397	Phase transformation in quenched mesomorphic isotactic polypropylene. Polymer, 2001, 42, 7561-7566.	1.8	138
398	Time-resolved isothermal crystallization of absorbable PGA-co-PLA copolymer by synchrotron small-angle X-ray scattering and wide-angle X-ray diffraction. Polymer, 2001, 42, 8965-8973.	1.8	27
399	Hard and soft confinement effects on polymer crystallization in microphase separated cylinder-forming PEO-b-PS/PS blends. Polymer, 2001, 42, 9121-9131.	1.8	179
400	Time-resolved shear behavior of end-tethered Nylon 6–clay nanocomposites followed by non-isothermal crystallization. Polymer, 2001, 42, 9015-9023.	1.8	105
401	Temperature dependence of polymer crystalline morphology in nylon 6/montmorillonite nanocomposites. Polymer, 2001, 42, 09975-09985.	1.8	234
402	Crystallization studies of isotactic polypropylene containing nanostructured polyhedral oligomeric silsesquioxane molecules under quiescent and shear conditions. Journal of Polymer Science, Part B: Polymer Physics, 2001, 39, 2727-2739.	2.4	135
403	Structure and morphology development in syndiotactic polypropylene during isothermal crystallization and subsequent melting. Journal of Polymer Science, Part B: Polymer Physics, 2001, 39, 2982-2995.	2.4	30
404	Morphology development during isothermal crystallization. II. Isotactic and syndiotactic polypropylene blends. Journal of Polymer Science, Part B: Polymer Physics, 2001, 39, 1876-1888.	2.4	23
405	Time-resolved crystallization study of absorbable polymers by synchrotron small-angle X-ray scattering. Journal of Polymer Science, Part B: Polymer Physics, 2001, 39, 153-167.	2.4	23
406	Primary Nucleation in Polymer Crystallization. Macromolecular Rapid Communications, 2001, 22, 611-615.	2.0	26
407	Title is missing!. Journal of Materials Science, 2001, 36, 3071-3077.	1.7	31
408	DETERMINATION OF CRYSTALLINE LAMELLAR THICKNESS IN POLY(ETHYLENE TEREPHTHALATE) USING SMALL-ANGLE X-RAY SCATTERING AND TRANSMISSION ELECTRON MICROSCOPY*. Journal of Macromolecular Science - Physics, 2001, 40, 625-638.	0.4	33
409	Molecular dynamics and microstructure development during cold crystallization in poly(ether-ether-ketone) as revealed by real time dielectric and x-ray methods. Journal of Chemical Physics, 2001, 115, 3804-3813.	1.2	59
410	Dislocation-Controlled Perforated Layer Phase in a PEO- b-PS Diblock Copolymer. Physical Review Letters, 2001, 86, 6030-6033.	2.9	63
411	Nanoscale reinforcement of polyhedral oligomeric silsesquioxane (POSS) in polyurethane elastomer. Polymer International, 2000, 49, 437-440.	1.6	182
412	Structure development during melt spinning and subsequent annealing of polybutene-1 fibers. Journal of Polymer Science, Part B: Polymer Physics, 2000, 38, 1872-1882.	2.4	49
413	Morphology development during isothermal crystallization. I. Isotactic and atactic polypropylene blends. Journal of Polymer Science, Part B: Polymer Physics, 2000, 38, 2580-2590.	2.4	31
414	Novel image analysis of two-dimensional X-ray fiber diffraction patterns: example of a polypropylene fiber drawing study. Journal of Applied Crystallography, 2000, 33, 1031-1036.	1.9	72

#	Article	IF	CITATIONS
415	Synthesis and Characterization of Segmented Polyurethanes Containing Polyhedral Oligomeric Silsesquioxanes Nanostructured Molecules. High Performance Polymers, 2000, 12, 565-571.	0.8	74
416	Structural and Morphological Inhomogeneity of Short-Chain Branched Polyethylenes in Multiple-Step Crystallization. Journal of Macromolecular Science - Physics, 2000, 39, 317-331.	0.4	10
417	Morphological Changes During Crystallization and Melting of Polyoxymethylene Studied by Synchrotron X-Ray Scattering and Modulated Differential Scanning Calorimetry. Journal of Macromolecular Science - Physics, 2000, 39, 519-543.	0.4	12
418	Probing the Early Stages of Melt Crystallization in Polypropylene by Simultaneous Small- and Wide-Angle X-ray Scattering and Laser Light Scattering. Macromolecules, 2000, 33, 978-989.	2.2	154
419	Crystallization Behavior of Poly(ethylene oxide) and Its Blends Using Time-Resolved Wide- and Small-Angle X-ray Scattering. Macromolecules, 2000, 33, 4842-4849.	2.2	66
420	In-Situ Simultaneous Synchrotron Small- and Wide-Angle X-ray Scattering Measurement of Poly(vinylidene fluoride) Fibers under Deformation. Macromolecules, 2000, 33, 1765-1777.	2.2	124
421	Crystallization Temperature-Dependent Crystal Orientations within Nanoscale Confined Lamellae of a Self-Assembled Crystallineâ^'Amorphous Diblock Copolymer. Journal of the American Chemical Society, 2000, 122, 5957-5967.	6.6	387
422	Structure Development during Shear Flow-Induced Crystallization of i-PP:  In-Situ Small-Angle X-ray Scattering Study. Macromolecules, 2000, 33, 9385-9394.	2.2	465
423	Phase structures and morphologies determined by competitions among self-organization, crystallization, and vitrification in a disordered poly(ethylene oxide)-b-polystyrene diblock copolymer. Physical Review B, 1999, 60, 10022-10031.	1.1	125
424	Crystal structure changes during isothermal crystallization, cooling and heating of linear polyethylene. Journal of Polymer Research, 1999, 6, 167-173.	1.2	13
425	Effect of miscible polymer diluents on the development of lamellar morphology in poly(oxymethylene) blends. Journal of Polymer Science, Part B: Polymer Physics, 1999, 37, 3115-3122.	2.4	29
426	Structure and Morphology Changes in Absorbable Poly(glycolide) and Poly(glycolide-co-lactide) during in Vitro Degradation. Macromolecules, 1999, 32, 8107-8114.	2.2	128
427	Isothermal Thickening and Thinning Processes in Low-Molecular-Weight Poly(ethylene oxide) Fractions Crystallized from the Melt. 8. Molecular Shape Dependence§. Macromolecules, 1999, 32, 4784-4793.	2.2	41
428	Interactions between Crystalline and Amorphous Domains in Semicrystalline Polymers:Â Small-Angle X-ray Scattering Studies of the Brill Transition in Nylon 6,6. Macromolecules, 1999, 32, 5594-5599.	2.2	64
429	Structure Development during the Melt Spinning of Polyethylene and Poly(vinylidene fluoride) Fibers by in Situ Synchrotron Small- and Wide-Angle X-ray Scattering Techniques. Macromolecules, 1999, 32, 8121-8132.	2.2	96
430	Crystallization and phase behavior in nylon 6/aromatic polyimide triblock copolymers. Macromolecular Chemistry and Physics, 1998, 199, 1107-1118.	1.1	24
431	Crystallization study of poly(ether ether ketone)/poly(ether imide) blends by real-time small-angle x-ray scattering. Journal of Macromolecular Science - Physics, 1998, 37, 365-374.	0.4	7
432	Time-resolved simultaneous SAXS/WAXS studies of peek during isothermal crystallization, melting, and subsequent cooling. Journal of Macromolecular Science - Physics, 1998, 37, 667-682.	0.4	16

#	Article	IF	CITATIONS
433	Melt crystalfization and crystal morphology of two low molecular weight linear polyethylene fractions. Journal of Macromolecular Science - Physics, 1997, 36, 553-567.	0.4	5
434	Dynamic Study of Crystallization- and Melting-Induced Phase Separation in PEEK/PEKK Blends. Macromolecules, 1997, 30, 4544-4550.	2.2	36
435	Solvent induced phase separation in a nylon 6-b-polyimide-b-nylon 6 triblock copolymer. Journal of Polymer Research, 1997, 4, 1-7.	1.2	11
436	Crystal morphological investigation in thin films of poly(aryl ether ketone ketone) having a meta-linkage. Polymer, 1997, 38, 5051-5058.	1.8	5
437	A.C. dielectric and TSC studies of constrained amorphous motions in flexible polymers including poly(oxymethylene) and miscible blends. Journal of Polymer Science, Part B: Polymer Physics, 1997, 35, 2121-2132.	2.4	33
438	Crystalline Homopolyimides and Copolyimides Derived from 3,3â€~,4,4â€~-Biphenyltetracarboxylic Dianhydride/1,3-Bis(4-aminophenoxy)benzene/1,12-Dodecanediamine. 2. Crystallization, Melting, and Morphology. Macromolecules, 1996, 29, 135-142.	2.2	35
439	Synthesis and Characterization of Poly(oxy-1,3-phenylenecarbonyl-1,4-phenylene) and Related Polymers. Macromolecules, 1996, 29, 6432-6441.	2.2	41
440	Isothermal Thickening and Thinning Processes in Low Molecular Weight Poly(ethylene oxide) Fractions Crystallized from the Melt. 5. Effect of Chain Defects. Macromolecules, 1996, 29, 8816-8823.	2.2	38
441	Microstructure and Phase Separation of Pekk, Pekk and their Blends. Materials Research Society Symposia Proceedings, 1996, 461, 33.	0.1	0
442	Miscibility and phase properties of poly(aryl ether ketone)s with three high temperature all-aromatic thermoplastic polyimides. Polymer, 1996, 37, 445-453.	1.8	26
443	Anomalous two-stage spherulite growth in poly(aryl ether ketones) during isothermal crystallization. Journal of Polymer Science, Part B: Polymer Physics, 1996, 34, 3095-3105.	2.4	7
444	Simple on-line x-ray setup to monitor structural changes during fiber processing. Journal of Applied Polymer Science, 1996, 62, 2061-2068.	1.3	25
445	Copolymer modification of nylon-6,6 with 2-methylpentamethylenediamine. Polymer, 1996, 37, 1217-1228.	1.8	15
446	SAXS studies of lamellar level morphological changes during crystallization and melting in PEEK. Polymer, 1996, 37, 5357-5365.	1.8	69
447	Time-resolved synchrotron X-ray study of crystalline phase transition in poly(aryl ether ketone) Tj ETQq1 1 0.7843 Polymer Physics, 1995, 33, 2439-2447.	814 rgBT / 2.4	Overlock 10 5
448	Effect of the heterogeneous distribution of lamellar stacks on amorphous relaxations in semicrystalline polymers. Polymer, 1995, 36, 2553-2558.	1.8	61
449	New Insight of Isothermal Melt Crystallization in Poly(aryl ether ether ketone) via Time-Resolved Simultaneous Small-Angle X-ray Scattering/Wide-Angle X-ray Diffraction Measurements. Macromolecules, 1995, 28, 6931-6936.	2.2	58
450	Crystal Morphology and Phase Identification in Poly(Aryl Ether Ketone)s and Their Copolymers. 4. Morphological Observations in PEKK with All p-Phenylene Linkages. Macromolecules, 1995, 28, 8855-8861.	2.2	6

#	Article	IF	CITATIONS
451	Crystalline Homopolyimides and Copolyimides Derived from 3,3',4,4'-Biphenyltetracarboxylic Dianhydride/1,3-Bis(4-aminophenoxy)benzene/1,12-Dodecanediamine. 1. Materials, Preparation, and Characterization. Macromolecules, 1995, 28, 6926-6930.	2.2	37
452	A laserâ€∎ided prealigned pinhole collimator for synchrotron x rays. Review of Scientific Instruments, 1994, 65, 597-602.	0.6	51
453	Crystallization study of a thermoplastic polyimide (new-TPI). Journal of Polymer Science, Part B: Polymer Physics, 1994, 32, 737-747.	2.4	31
454	Crystallization of poly(aryl ether ketone ketone) copolymers containing terephthalate/isophthalate moieties. Journal of Polymer Science, Part B: Polymer Physics, 1994, 32, 2585-2594.	2.4	30
455	Polymorphism in poly(aryl ether ketone)s. Polymer, 1994, 35, 2290-2295.	1.8	69
456	Crystal Structure, Morphology, and Phase Transitions in Aromatic Polyimide Oligomers. 1. Poly(4,4'-oxydiphenylene pyromellitimide). Macromolecules, 1994, 27, 989-996.	2.2	32
457	Crystal Morphology and Phase Identifications in Poly(aryl ether ketone)s and Their Copolymers. 1. Polymorphism in PEKK. Macromolecules, 1994, 27, 2136-2140.	2.2	63
458	Crystal Morphology and Phase Identifications in Poly(aryl ether ketone)s and Their Copolymers. 2. Poly(oxy-1,4-phenylenecarbonyl-1,3-phenylenecarbonyl-1,4-phenylenene). Macromolecules, 1994, 27, 5787-5793.	2.2	26
459	Miscibility of three different poly(aryl ether ketones) with a high melting thermoplastic polyimide. Polymer, 1993, 34, 3315-3318.	1.8	19
460	Time-resolved X-ray study of poly(aryl ether ether ketone) crystallization and melting behaviour: 1. Crystallization. Polymer, 1993, 34, 3986-3995.	1.8	157
461	Glass transition, crystallization, and morphology relationships in miscible poly(aryl ether ketones) and poly(ether imide) blends. Journal of Polymer Science, Part B: Polymer Physics, 1993, 31, 901-915.	2.4	110
462	Time-resolved X-ray study of poly(aryl ether ether ketone) crystallization and melting behaviour: 2. Melting. Polymer, 1993, 34, 3996-4003.	1.8	110
463	Isothermal thickening and thinning processes in low-molecular-weight poly(ethylene oxide) fractions crystallized from the melt. 4. End-group dependence. Macromolecules, 1993, 26, 5105-5117.	2.2	85
464	Structure, crystallization and morphology of poly (aryl ether ketone ketone). Polymer, 1992, 33, 2483-2495.	1.8	172
465	Isothermal crystallization kinetics of poly(ether ketone ketone) and its carbon-fibre-reinforced composites. Polymer, 1991, 32, 2799-2805.	1.8	54
466	Study of a thermotropic liquid-crystalline polyester at elevated pressures. Journal of Polymer Science, Part B: Polymer Physics, 1990, 28, 189-202.	2.4	14
467	The Effects of Temperature and Pressure on the Dynamic Longitudinal Volume Viscosity of Two Model Polymers. Journal of Rheology, 1988, 32, 533-553.	1.3	2
468	Continuous Production of Hollow Hydrogel Fibers with Graphene Inner Wall. Materials Science Forum, 0, 898, 2197-2204.	0.3	1